

Electronic Supplementary Information

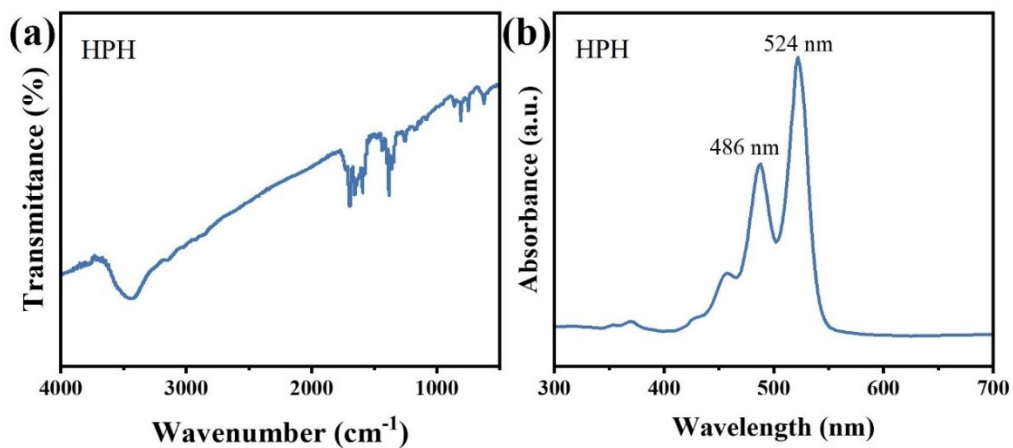
In-situ formed Copper Nanoparticles via Strong Electronic Interaction with Organic Skeleton for pH-Universal Electrocatalytic CO₂ Reduction

Ying Zhang,^{*a,1} Chenchen Zhang,^{a,1} Dan Wang,^a Jianing Gui,^a Junjun Mao,^a Yang Lou,^a Chensi Pan^a and Yongfa Zhu^a

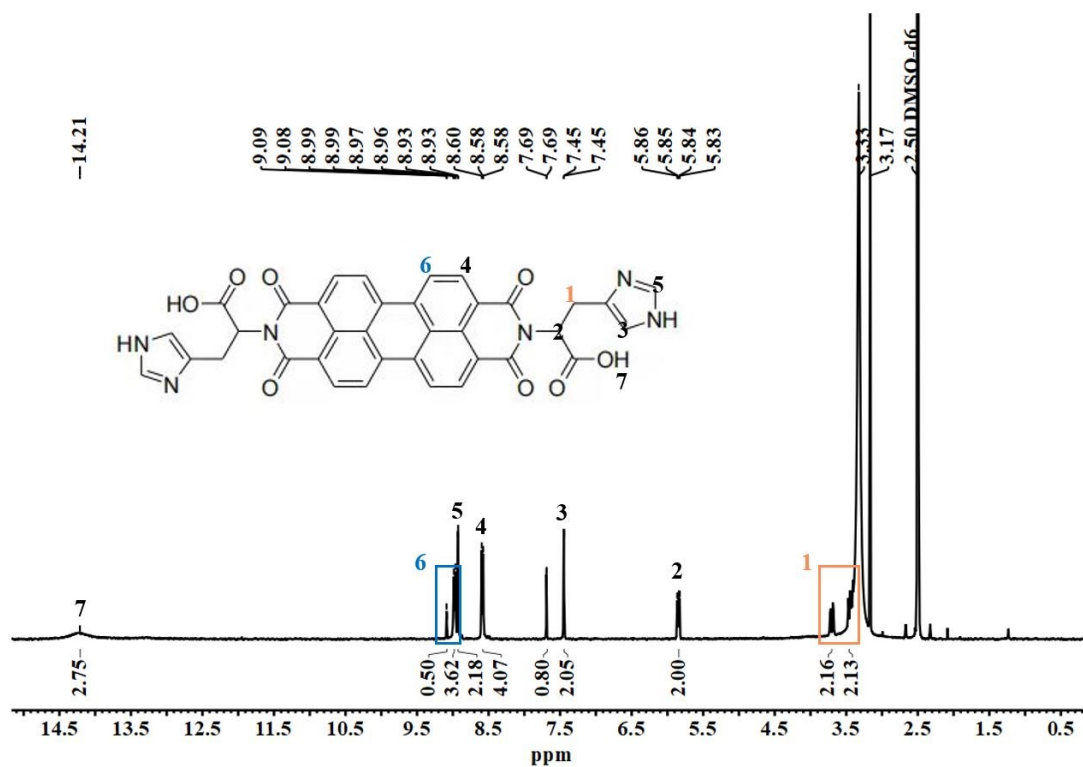
^aKey Laboratory of Synthetic and Biological Colloids, Ministry of Education, School of Chemical and Material Engineering, Jiangnan University, Wuxi, Jiangsu 214122, China

* To whom correspondence should be addressed.

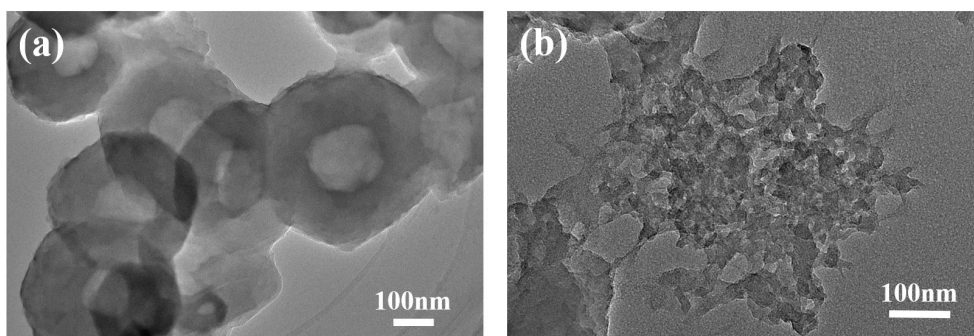
Email: ying.zhang@jiangnan.edu.cn



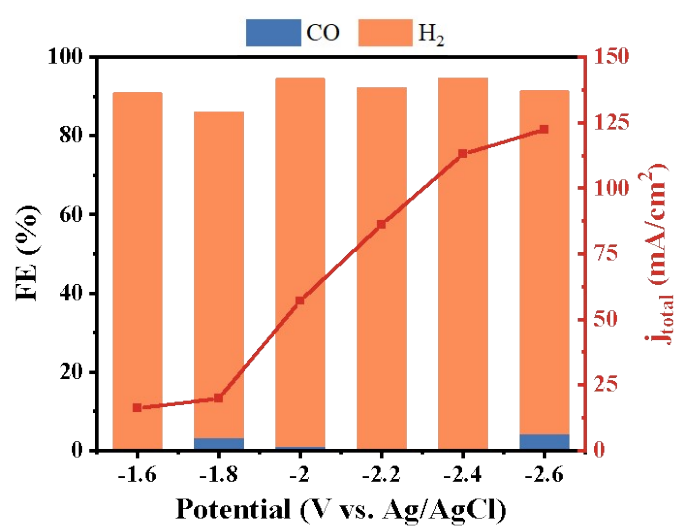
Supplementary Figure S1. (a) FTIR spectrum and (b) UV-vis absorption spectrum of HPH.



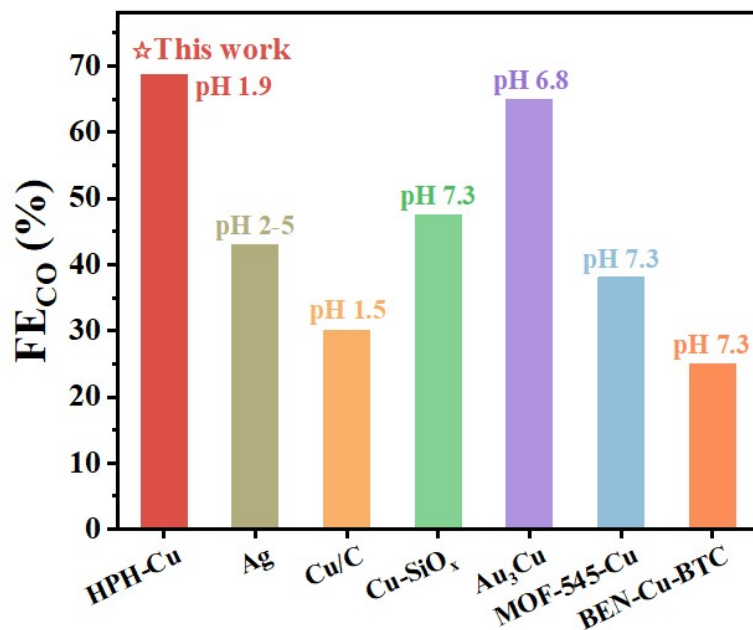
Supplementary Figure S2. ¹H-NMR spectrum of HPH in DMSO-d₆.



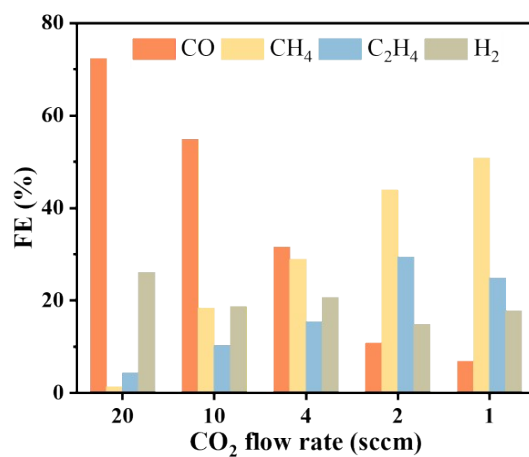
Supplementary Figure S3. TEM images of (a) HPH and (b) HPH-Cu.



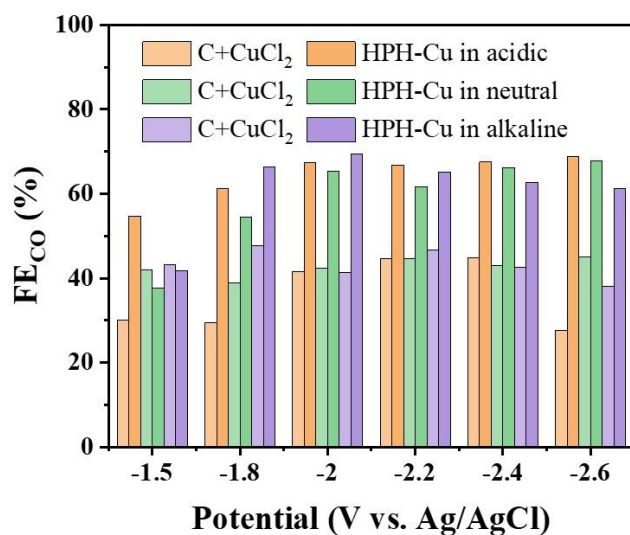
Supplementary Figure S4. FE and current densities of HPH at different applied potential.



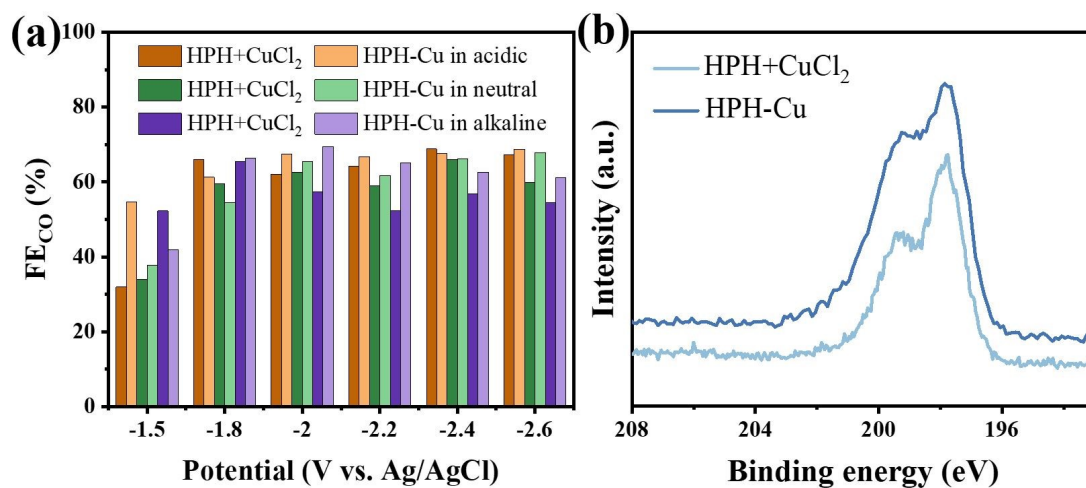
Supplementary Figure S5. Comparison of Faradaic efficiency of CO and pH of electrolyte with HPH-Cu and other reported CO₂RR catalysts.



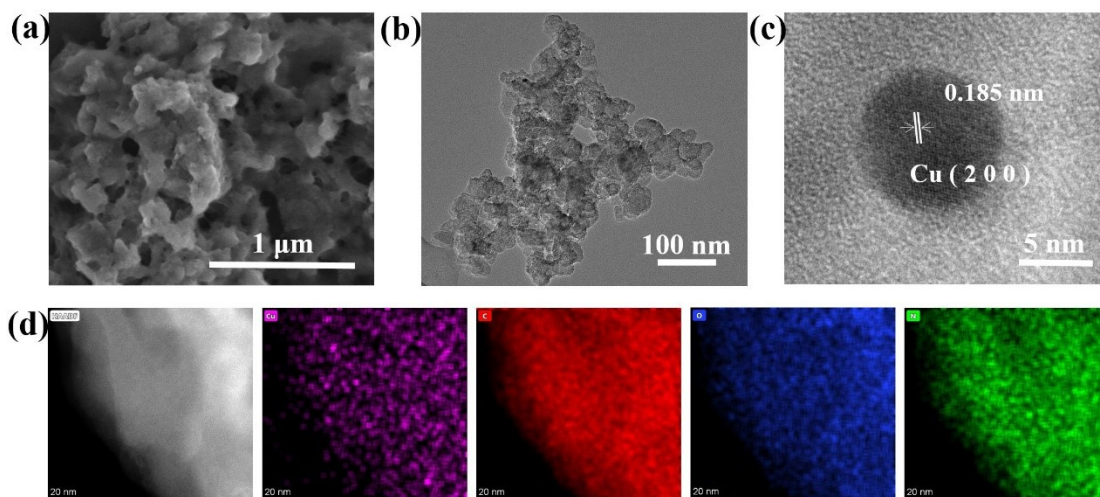
Supplementary Figure S6. FEs of HPH-Cu in acidic electrolytes at different CO₂ flow rates.



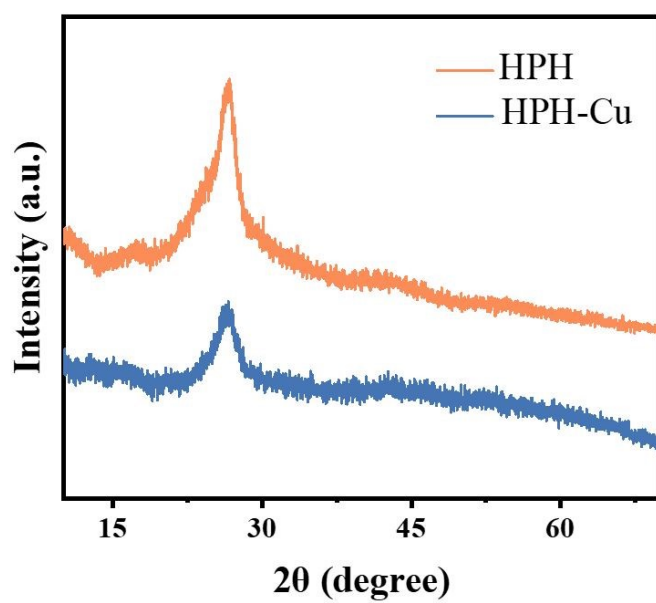
Supplementary Figure S7. FE_{CO} of HPH-Cu and C+CuCl₂ in acidic, alkaline and neutral electrolytes.



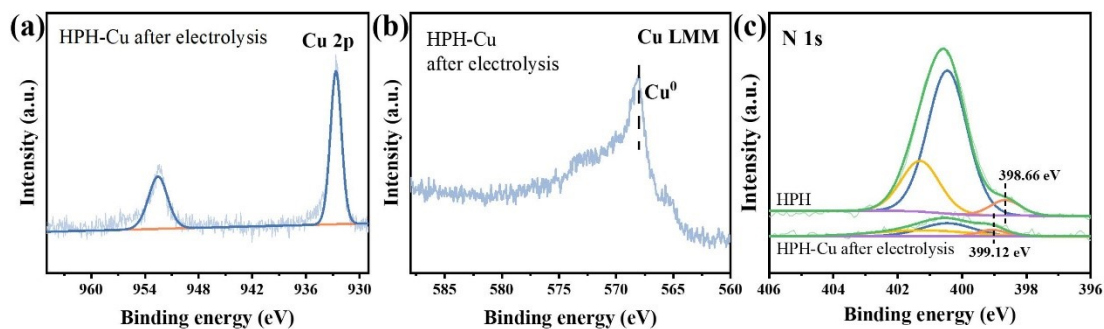
Supplementary Figure S8. (a) FE_{CO} of HPH-Cu and HPH+CuCl₂ in acidic, alkaline and neutral electrolytes; (b) Cl 2p XPS spectrum of HPH-Cu and HPH+CuCl₂.



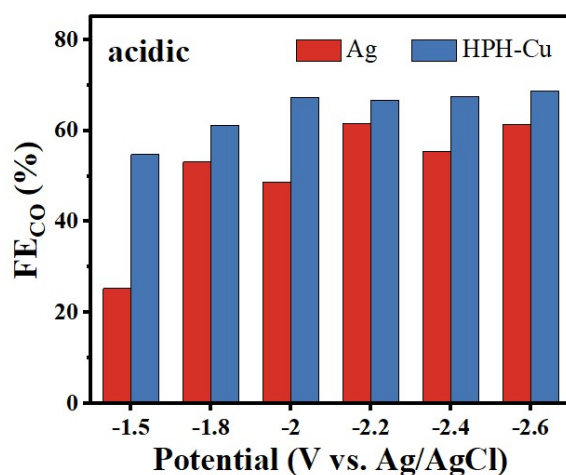
Supplementary Figure S9. (a) SEM image, (b) TEM image, (c) High-resolution TEM image and (d) Elemental mapping images of HPH-Cu after electrolysis.



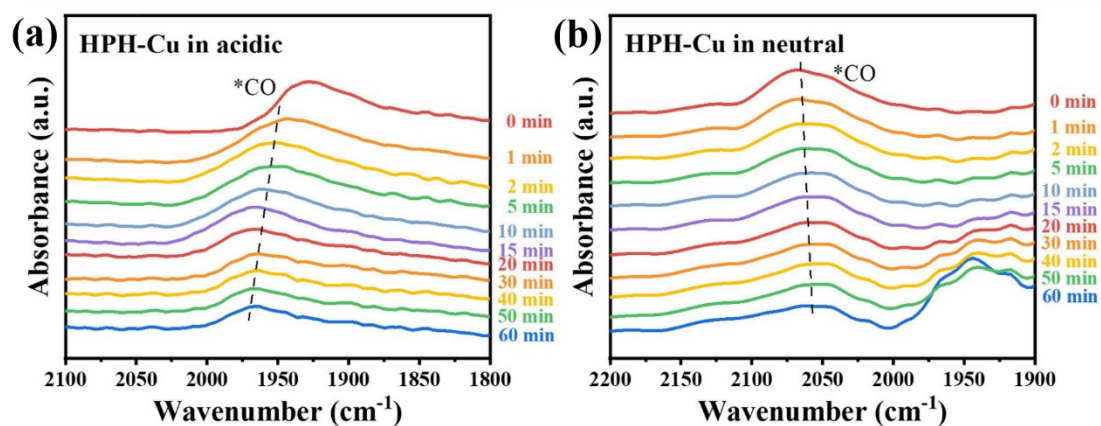
Supplementary Figure S10. XRD patterns of HPH and HPH-Cu.



Supplementary Figure S11. (a) Cu 2p and (b) Cu LMM XPS spectra of HPH-Cu after electrolysis; (c) XPS N 1s spectra of HPH and HPH-Cu after electrolysis.



Supplementary Figure S12. The FE_{CO} of HPH-Cu and Ag in acidic electrolyte.



Supplementary Figure S13. In situ ATR-SEIRAS spectra of CO desorption after -1.2 V vs. Ag/AgCl electrolysis in CO₂-saturated (a) acidic and (b) neutral electrolytes.

Supplementary Table S1. E (V vs. Ag/AgCl) after iR correction and E (V vs. RHE) after iR correction of HPH-Cu in acidic, alkaline, and neutral electrolytes.

	E (V vs. Ag/AgCl)	I/mA	R/ Ω	E (V vs. Ag/AgCl) after 80% iR correction	E (V vs. RHE) after 80% iR correction
acidic	-1.5	28.19	3	-1.43	-1.13
	-1.8	84.82	3	-1.60	-1.30
	-2.0	102.70	3	-1.75	-1.45
	-2.2	147.30	3	-1.85	-1.55
	-2.4	180.98	3	-1.97	-1.67
	-2.6	207.36	3	-2.10	-1.80
alkaline	-1.5	44.59	1	-1.46	-0.46
	-1.8	127.29	1	-1.70	-0.70
	-2.0	193.93	1	-1.84	-0.84
	-2.2	250.23	1	-2.00	-1.00
	-2.4	378.37	1	-2.10	-1.10
	-2.6	408.63	1	-2.27	-1.27
neutral	-1.5	19.55	3	-1.45	-0.85
	-1.8	59.50	3	-1.66	-1.06
	-2.0	88.18	3	-1.79	-1.19
	-2.2	123.85	3	-1.90	-1.30
	-2.4	200.58	3	-1.92	-1.32
	-2.6	160.68	3	-2.21	-1.61

Supplementary Table S2. Cu content analysis result of HPH-Cu.

Sample	m_0 (g)	Test element	Element content W (%)
HPH-Cu	0.0659	Cu	7.12%

Supplementary Table S3. Detailed comparison of Faradaic efficiency of CO and pH of electrolyte with HPH-Cu and other reported CO₂RR catalysts.

Catalyst	Electrolyte	Faradaic efficiency		Reference
		pH	of CO [%]	
HPH-Cu	0.45 M K ₂ SO ₄ + 0.05 M H ₂ SO ₄	1.9	68	☆this work
Ag	polymer electrolytes	2~5	43	<i>Nat Chem</i> , 2021, 13 , 33-40.
Cu/C	0.4 M K ₂ SO ₄ + 0.1 M H ₂ SO ₄	1.5	30	<i>Nat Catal</i> , 2022, 5 , 268-276.
Cu-SiOx	0.1 M KHCO ₃	7.3	47.5	<i>Nat commun</i> , 2021, 12 , 2808.
Au ₃ Cu NPs	0.1 M KHCO ₃	6.8	65	<i>Nat commun</i> , 2014, 5 , 4948.
MOF-545-Cu	0.1 M KHCO ₃	7.3	38	<i>Chin Chem Lett</i> , 2023, 34 , 107458.
BEN-Cu-BTC	0.1 M KHCO ₃	7.3	25	<i>Catal Sci Technol</i> , 2019, 9 , 5668-5675.